REPORT DOCUMENTATION PAGE

Form Approved OMB NO. 0704-0188

1. REPORT DATE (DD-MM-YYYY)	2. REPORT TYPE	3. DATES COVERED (From - To)
22-01-2017	Final Report	30-Sep-2012 - 30-Sep-2016

4. TITLE AND SUBTITLE
Final Report: Time-Frequency and Non-Laplacian Phenomena at Radio Frequencies

5a. CONTRACT NUMBER
W911NF-12-1-0526

5b. GRANT NUMBER

5c. PROGRAM ELEMENT NUMBER
611102

6. AUTHORS
Michael Steer

5d. PROJECT NUMBER

5e. TASK NUMBER

5f. WORK UNIT NUMBER

7. PERFORMING ORGANIZATION NAMES AND ADDRESSES
North Carolina State University
2701 Sullivan Drive
Admin Srvcs III, Box 7514
Raleigh, NC 27695 -7514

8. PERFORMING ORGANIZATION REPORT NUMBER

9. SPONSORING/MONITORING AGENCY NAME(S) AND ADDRESS (ES)
U.S. Army Research Office
P.O. Box 12211
Research Triangle Park, NC 27709-2211

10. SPONSOR/MONITOR'S ACRONYM(S)
ARO

11. SPONSOR/MONITOR'S REPORT NUMBER(S)
62321-EL.7

12. DISTRIBUTION AVAILIBILITY STATEMENT
Approved for Public Release; Distribution Unlimited

13. SUPPLEMENTARY NOTES
The views, opinions and/or findings contained in this report are those of the author(s) and should not contrued as an official Department of the Army position, policy or decision, unless so designated by other documentation.

14. ABSTRACT
There are non-stationary radio frequency signals that are very difficult to detect using conventional equipment and difficult to analyze using conventional techniques. Most of our receiver, measurement and analysis technology is based on an underlying assumption that a signal being received is stationary. Key to the ability to examine such signals was the development of a scheme, reported here, for detecting very small signals close in frequency to a large signal using only power measurements. A measurement system was implemented that used a detection algorithm based on power measurements rather than voltage measurements. The system was used to measure a

15. SUBJECT TERMS
radio frequency, chaos, vibrating antenna, co-site interference

16. SECURITY CLASSIFICATION OF:			17. LIMITATION OF ABSTRACT	15. NUMBER OF PAGES	19a. NAME OF RESPONSIBLE PERSON
a. REPORT	b. ABSTRACT	c. THIS PAGE			Michael Steer
UU	UU	UU	UU		19b. TELEPHONE NUMBER 919-515-5191

RPPR

as of 01-Nov-2017

Agency Code:

Proposal Number: **Agreement Number:**

Organization:
Address: , ,
Country:
DUNS Number: EIN:
Report Date: Date Received:
for Period Beginning and Ending
Title:
Begin Performance Period: **End Performance Period:**
Report Term: -
Submitted By: Email:
Phone:

Distribution Statement: -

STEM Degrees: **STEM Participants:**

Major Goals:

Accomplishments:

Training Opportunities:

Results Dissemination:

Plans Next Period:

Honors and Awards:

Protocol Activity Status:

Technology Transfer:

Final Report

Time-Frequency and Non-Laplacian Phenomena at Radio Frequencies

U.S. Army Research Office grant W911NF-12-1-0526

Michael B. Steer

Department of Electrical and Computer Engineering, North Carolina State University

Contents

1. Introduction

The premise of this project was that there are non-stationary signals that are very difficult to detect using conventional detection equipment. This includes receivers which detected correlated signals, and modern spectrum analyzers which respond to voltages rather than the peak signals of earlier detection signals. Many military listening devices assume that a signal being received is stationary. For example a communication signal is a modulated carrier signal and while not being absolutely stationary it can be detected using a stationary assumption as on average, that is after a dwell interval, the signal can be treated as stationary. Other unintended emissions such as a leaking clock signal are stationary and even very low-level such signals can be detected. Key to the ability to examine such signals was the development of a scheme for detecting very small signals close in frequency to a large signal using only power measurements. This was based on an earlier measurement system but enhancements were made to the detection algorithm which better responded to power than voltage. The system was used to measure a reflected radar signal from vibrating objects which has small Doppler-like sidebands.

This work attempted to detect noise signals and chaotic signals. We over reached, that is for sure, as detection of such a signal proved particularly elusive. We did write two journal papers from the work performed under the sponsorship of this project but much remains to be done. Prior to the project we had established the world record for detecting small signals close in frequency to a large signal. In this project we enhanced this work and in particular developed a way of measuring such signals even if they were non-stationary. The first paper describes the measurement scheme and the second paper applied the work to the measurement of radar reflections form a chaotically vibrating antenna. When an antenna vibrates it is nearly always a chaotic vibration. Or in the preferred language of chaos investigators the antenna vibrations have non-stationary nonlinear dynamic behavior. This description is preferred because there are many “chaotic” behaviors and calling something chaotic implies that the behavior is reasonably well understood. The journal paper on measurements of a chaotically vibrating antenna provides a compact description.

This report focuses on the results of the research that are not represented by or not fully described by the papers.

2. Current Signal Identification of Radio Frequency Circuits

This project undertook the investigation of nonstationary phenomena at radio and microwave frequencies. The work was based on the premise that the analysis and simulation tools developed for our understanding of RF and microwave electronics and signals in general assume that the signals are stationary and that electronic phenomena is governed by integer calculus. The project undertook the investigation of analyzing signals and simulating electronics circuits without necessarily using integer calculus. The signals in circuits described by integer calculus are deterministic and stationary. Signals such as chaotic signals, the generation of which always seems to require nonlinear feedback in a circuit, are deterministic but a not stationary. Thermal noise is a signal that is neither deterministic nor stationary but our detection of noise assume

certain statistics. It is not clear that we have any ability to detect signals that do not have simple statistics, are non-stationary, and are not deterministic. The research report here made the first in-roads but much remains to be done.

Analysis of all virtually all electronics, and not just RF and microwave electronics, is based on the concept that signals are stationary and circuits act deterministically. There are a couple of exceptions. Very simple chaotic circuits have been considered previously. These are circuits that generally have a few reactive elements and just one nonlinear resistive element. What is known as the Chua circuit is one such circuit. Most of the investigations seemed to address how such a simple circuit could have such widely varying responses with small changes in parameters.

Our ability to exploit the physical environment either through sensing or communications, for example, is largely based on partitioning of the physical space into discrete physical effects and advances in detection driven by signal processing enhancements. Domain views, such as either the frequency-domain or time-domain views, are used to simplify the effort required to understand physical responses. There are other views such as the wavelet-domain which facilitate the understanding of phenomenology simultaneously localized in frequency and time. Domain views simplify a problem by retaining essential aspects and discarding nonessential aspects. For example, in the frequency domain view transient responses are dispensed with and only the steady state response is retained. There may be other domain views that are ideally suited to detecting responses from probed targets that could include nonlinear responses or memory-effect responses.

Another example of our inability to understand the way the world works is the poor state of speech recognition. While a speech recognition was not an outcome of this research, it is likely that the way we are going about solving this particular problem is not correct. Could it be that we are trying to force a particular solution on a behavior which simply cannot be resolved using our current analysis approaches. The brain surely does not do arithmetic with complex numbers. There must be other ways to process signals and these should be inherently simple ways at that. We need different ways of processing and extracting information. Are we making the same mistake in trying to force a particular solution on electronic signals emanating from sources that do not have origins in well-behaved integer calculus as well as signals that are inherently non stationary.

3. Oscillator Analysis

The project began with the expectation that we could show that phase noise on oscillators was due to a chaotic process. The author of this report still believes that it is but was not able to demonstrate that in this project. Our investigations were hampered by the phase noise being so low in modern oscillators. The circuit we were using to provide experimental data was a state-of-the-art voltage-controlled oscillator centered at 5.3 GHz. The noise was too low to capture using a real-time oscilloscope, and a belief was established that frequency-domain measurements perhaps were not valid in measuring the power of a non-stationary signal. The task reported here

was the development of a relatively simple model of the oscillator that could be used in analysis. The 5 GHz Oscillator is shown in Figure 1. MATLAB-based simulations were undertaken and each simulation required about 1 week of computing time. These simulations were performed as part of a ARO STIR project are reported elsewhere, see the final report for the USARO grant W911NF-15-1-0567.

This section provides sufficient information to use the simplified model in future research.

3.1 Extraction of Oscillator Model

Extraction of a useable simple model of an oscillator from a full blown circuit model necessitates an understanding of the way the oscillator was designed. The majority of microwave oscillators are Colbitts oscillators operating as admittance oscillators with negative conductance. As the oscillation signal level increases the net conductance, the sum of the nonlinear conductance and the load conductance goes to zero as the nonlinear conductance increases with increasing amplitude. Ideally, to avoid multi-frequency oscillation, the active device conductance is independent of signal level. These characteristics are shown in Figure 2.

While designing a stable voltage controlled oscillator, ideally we expect the device parameters to be dependent only on the amplitude of the oscillations as shown in Figure 2 and the resonator parameters to be dependent only on the angular frequency of the oscillations. The design of a reflection oscillator involves in matching the inverse reflection coefficient of the active device to the reflection coefficient of the resonator: $1/\Gamma_d = \Gamma_r$ or $\Gamma_{d*}\,\Gamma_r = 1$

Achieving this condition at radio frequencies over an entire bandwidth range is difficult, as at higher frequencies, the parasitics in the circuit are very significant and complicate straightforward design. The oscillator must satisfy the stability criterion over the entire tuning range maintaining the output power constant and phase noise low. This oscillator implements a scheme that compensates for the effect of the parasitics by embedding a network that modifies the effective active device reflection coefficient and enables one port oscillator design techniques to be used.

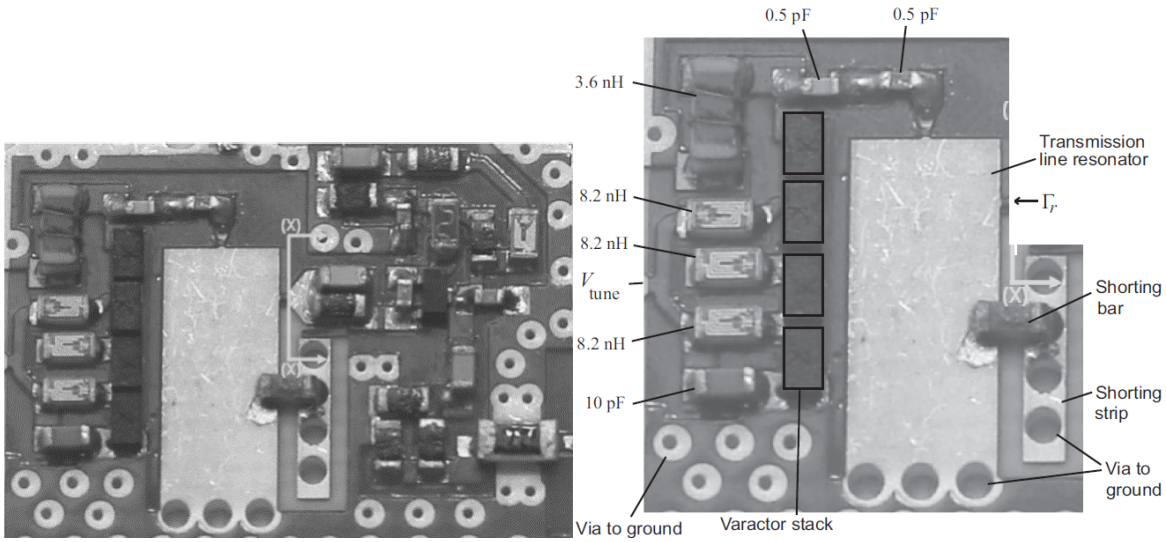

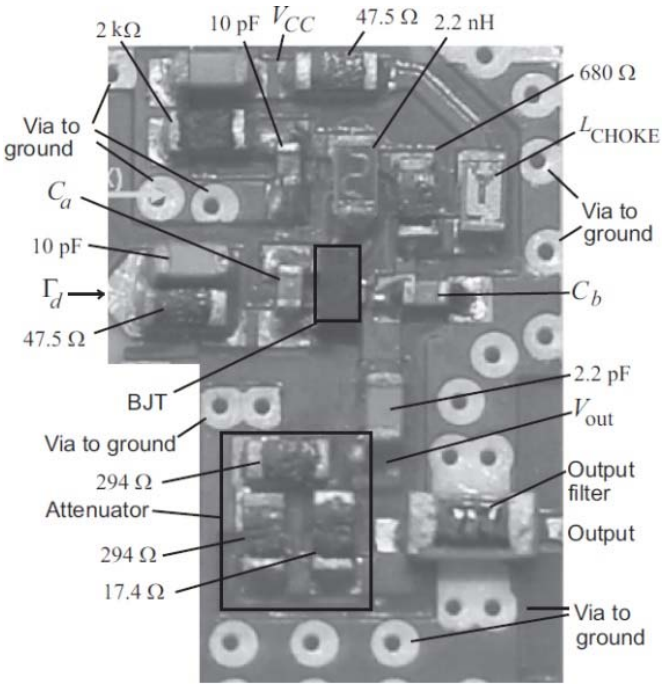

(c)

Figure 1: C-band VCO circuit: (a) complete oscillator with the resonator network to the left of the cutaway line (x-x) separated from the active circuit to the right; (b) annotated resonator network; and (c) annotated active network. The Pi attenuator (with 294 Ω resistors in the shunt legs and a 17.4 Ω series resistor) is between V_{out} and the 50 Ω bandpass filter.

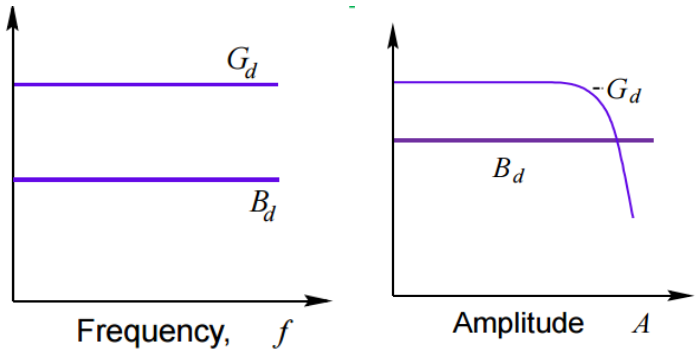

Figure 2 Variation of the device parameters with respect to Frequency and Amplitude in ideal scenario.

While designing negative resistance oscillators, we use Kurokawa's one-port oscillator stability requirement. To apply this one port criterion, each of the networks-the active device, resonator, and device termination are characterized as one-ports.

If the device with admittance $Y_d = G_d + jB_d$ is connected to a resonator of admittance $Y_r = G_r + jB_r$, the conditions required for oscillation can be determined at equilibrium as follows:

$G_d(A) = G_r(\omega)$ $\quad$ $B_d(A) = B_r(\omega)$

where, A is the voltage amplitude and ω is the angular frequency at equilibrium.

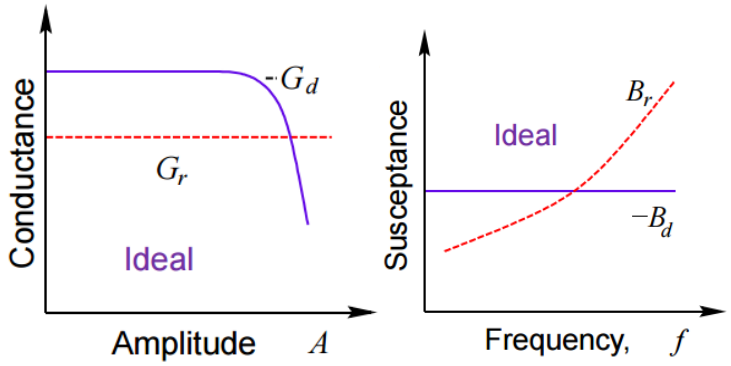

Figure 3: Intersection of the admittance loci of the device and resonator network.

These conditions can be graphically represented by taking the negative of the device's admittance i.e $-Y_d(A) = -G_d(A) - jB_d(A)$ and the locus of the resonator's admittance i.e. $Y(\omega) = G_r(\omega) + jB_r(\omega)$ as shown in Figure 3. In order to achieve stable single frequency oscillations, the intersection of this inverse device reflection coefficient locus and the resonator admittance locus in the complex plane must occur at a single point. Stability issues will occur if there are multiple intersections, which results in multiple oscillations, oscillator start-up problems and unwanted noise. For an oscillator which operates over a range of frequencies, as the circuit parasitics

significantly affect the tuning behavior, the device parameters would be frequency dependent. Thus, the device admittance should now be described as $-Y_d(A,\omega)$.

3.2 Description of the Oscillator

The design objective of the oscillator in Figure 4 is the generation of a frequency independent negative conductance $G_d(A, \omega)$ with a prescribed reflection coefficient shape Γ_d using a transistor in common base configuration with series inductive feedback. The effective device conductance is modified when there is reactive loading, due to which it becomes frequency dependent.

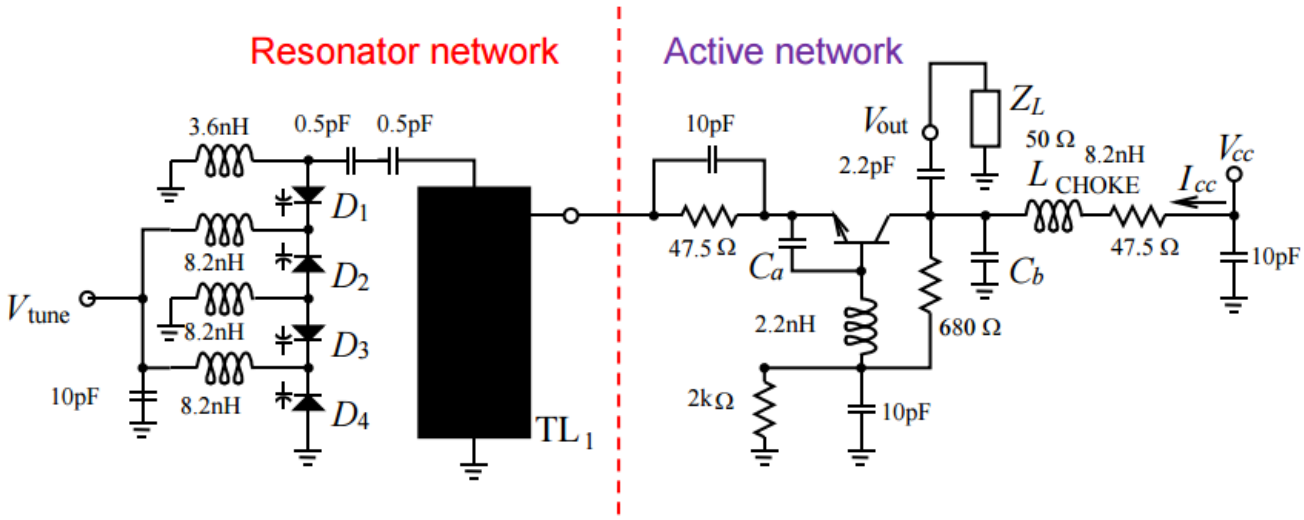

Figure 4 Tunable SiGe BJT VCO

A negative conductance oscillator is realized using a series inductor in the base lead. The base inductance provides the required negative feedback between the input and output of the transistor which results in a negative conductance from the emitter to the ground. Since the feedback is frequency dependent, this induced negative conductance is also frequency dependent. The reactive loading by the capacitors C_a and C_b, which are chosen by reflection coefficient shaping, modifies the effective device conductance so that it now becomes frequency independent. The resonator network is resonant at a frequency above the oscillation frequency, so it presents an inductance at the oscillation frequency. The resonator network consists of a transmission line which is coupled to stack of four varactors which provides variable capacitance.

3.3 Transformation into Colpitts Oscillator

3.3.1 Theoretical Explanation

All oscillators can be classified as either negative resistance oscillators (reflection oscillator) or feedback oscillators. The distinguishing criterion is whether there is an obvious feedback circuit (a distinct feedback block) . At Radio frequencies, it becomes difficult to construct a feedback circuit without introducing excess phase shift. Therefore, almost all oscillators in the radio frequency range are classified as negative resistance oscillators.

In a negative resistance oscillator model, oscillators are represented as a combination of an active element and a passive element. The active element generates negative resistance and drives the passive element, which is usually a resonator. When the negative resistance beats all losses in the resonator as well as the active element, oscillation builds up. Even though the negative resistance analysis is so common, still there are questions regarding the validity of this analysis. Also, some important oscillation parameters like loaded-*Q* cannot be derived from this analysis. Loaded-*Q* is one of the most important fundamental parameters because it dictates spectral purity i.e phase noise.

On the other hand, the feedback model of an oscillator is known to give better insights into oscillation performance. Although building an obvious feedback circuit is almost impossible at radio frequencies, interpreting a negative resistance oscillator using the feedback model is possible. This transformation enables transmission analysis of RF and microwave oscillators that are otherwise treated with the negative resistance model.

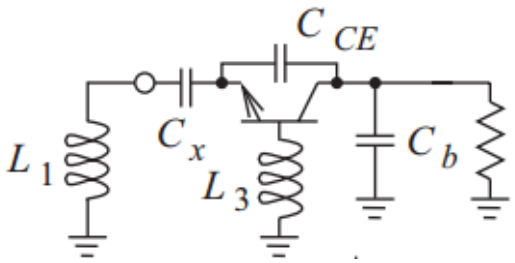

Figure 5: Replacing the resonator network with equivalent inductance

In the Figure 4 voltage controlled oscillator, we know that the resonator network resonates at a frequency above the frequency of oscillation. So, the resonator would present an inductance to the active network at the frequency of oscillation. Thus, the resonator can be replaced by an equivalence inductor as shown in Figure 5 at the oscillation frequency. Here the capacitance C_x is the equivalent capacitance which is obtained from the capacitance C_a and base-emitter parasitics. The C_{CE} i.e. the collector-emitter capacitance is one of the dominant parasitic capacitances which contribute to the feedback network.

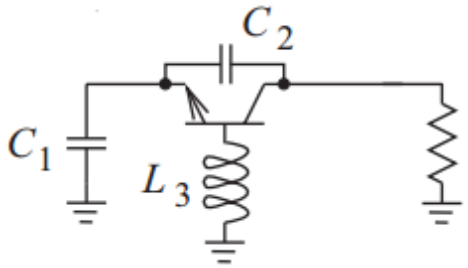

Figure 6 Combining the elements**.**

The inductor L_1, which is the equivalent of the resonator network, and the equivalent capacitance C_x can be combined to form a capacitance C_1 at the emitter. The collector-emitter parasitic capacitance can be written as capacitance C_2. This simplification is shown in the Figure 6.

Now, as all the feedback elements C_1, C_2 and L_3 are obtained, we can replace the transistor by an amplifier block and we can represent this as a feedback oscillator as shown in Figure 7. Thus, the reflection coefficient voltage controlled oscillator is simplified into a basic feedback oscillator with amplifier stage and feedback network.

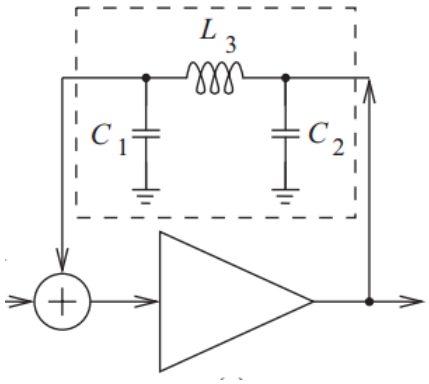

Figure 7 Final feedback form.

3.3.2 Derivation from transistor model

The above derived feedback form can be extracted for the voltage controlled oscillator. To start with, we first obtain the transistor model with all the parasitics listed in the Figure 8.

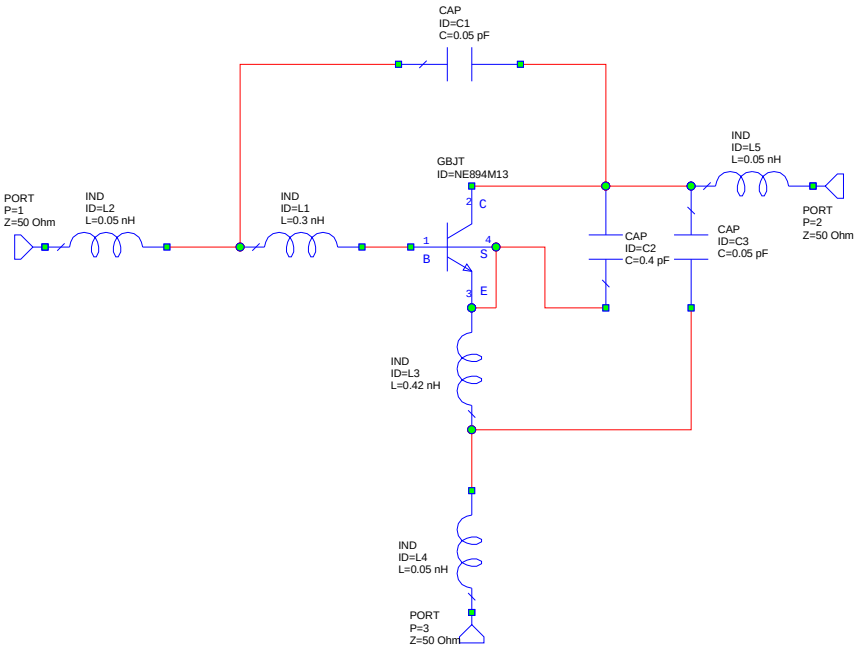

Figure 8: NE894M13 Si BJT transistor model with all parasitics.

From the model we can list the parasitics as: C_{CE} = 0.05 pF, C_{CB} = 0.01 pF, C_{CBPKG} = 0.05 pF, C_{CEPKG} = 0.05 pF, L_E = 0.42nH, L_B = 0.3 nH, L_{EPKG} = 0.05 nH, L_{CPKG} = 0.05nH, L_{BPKG} = 0.05nH. The value of the capacitors C_a and C_b is 0.5pF which are obtained from reflection coefficient shaping. With the VCO tuned for 5.3 GHz oscillation the other parameters of the simple circuit are C_1 = 1.8 pF, C_2 = 0.68 pF, L_3 = 2.2nH.

3.3.3 Summary

From the theoretical extraction and hand calculations we have obtained the values of the feedback elements as C_1=1.8pF, C_2=0.68pF and L_3=2.2nH. Now using these values as starting point, we can build up the System Level Oscillator and then modify the values accordingly using AWR simulations as yardstick to match this to the Voltage Controlled Oscillator.

3.3.4 Simulation of Complete Oscillator Model

The complete oscillator model agrees very well with measurements of the fabricated oscillator. In this study the simplified model was derived to match the simulated results from the performance of the full oscillator model. Both were tuned for 5.3 GHz operation. This subsection reports the simulated results obtained using harmonic balance simulation of he full VCO circuit and the simplified model of the oscillator tuned for 5.3 GHz operation. The full oscillator model is given in Figure 9. Key simulated results are shown in Figures 10 to 13.

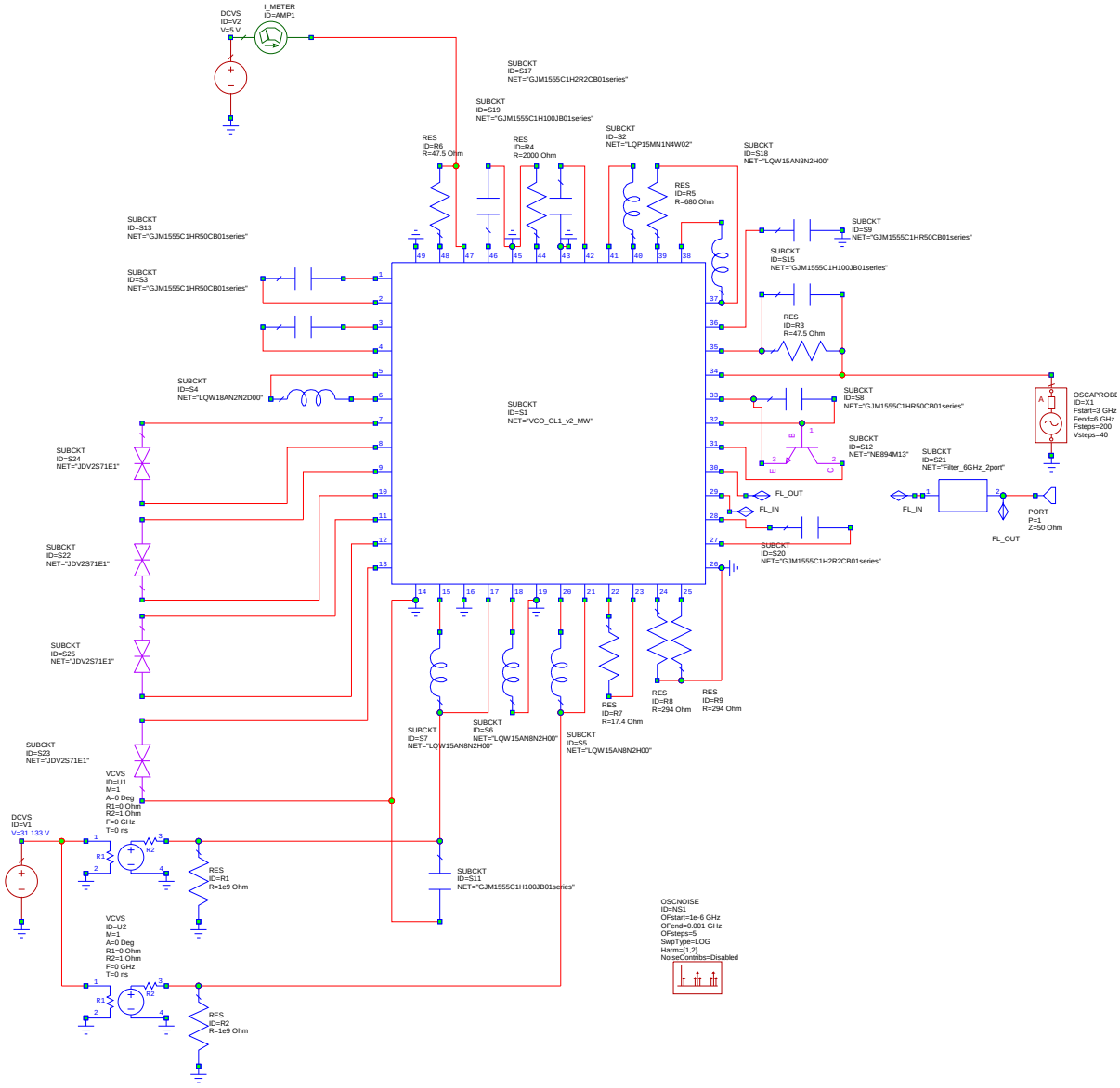

Figure 9: Complete VCO circuit schematic in AWR.

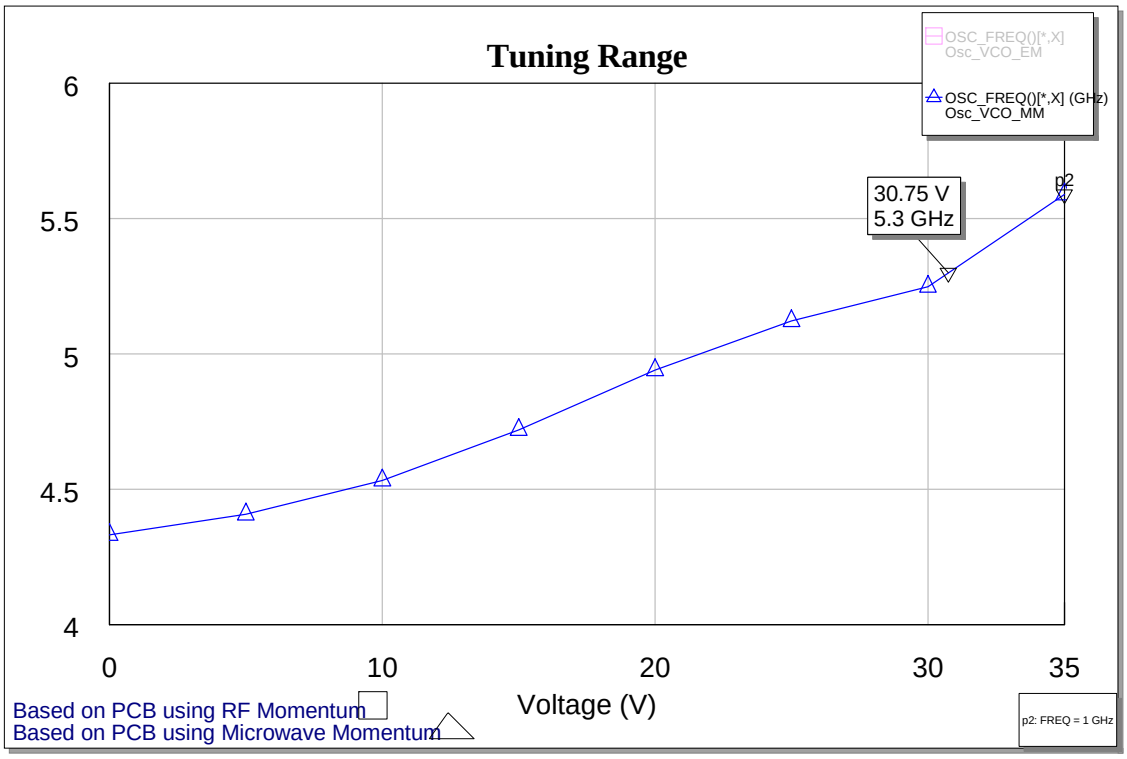

Figure 10: Tuning Range of the Oscillator

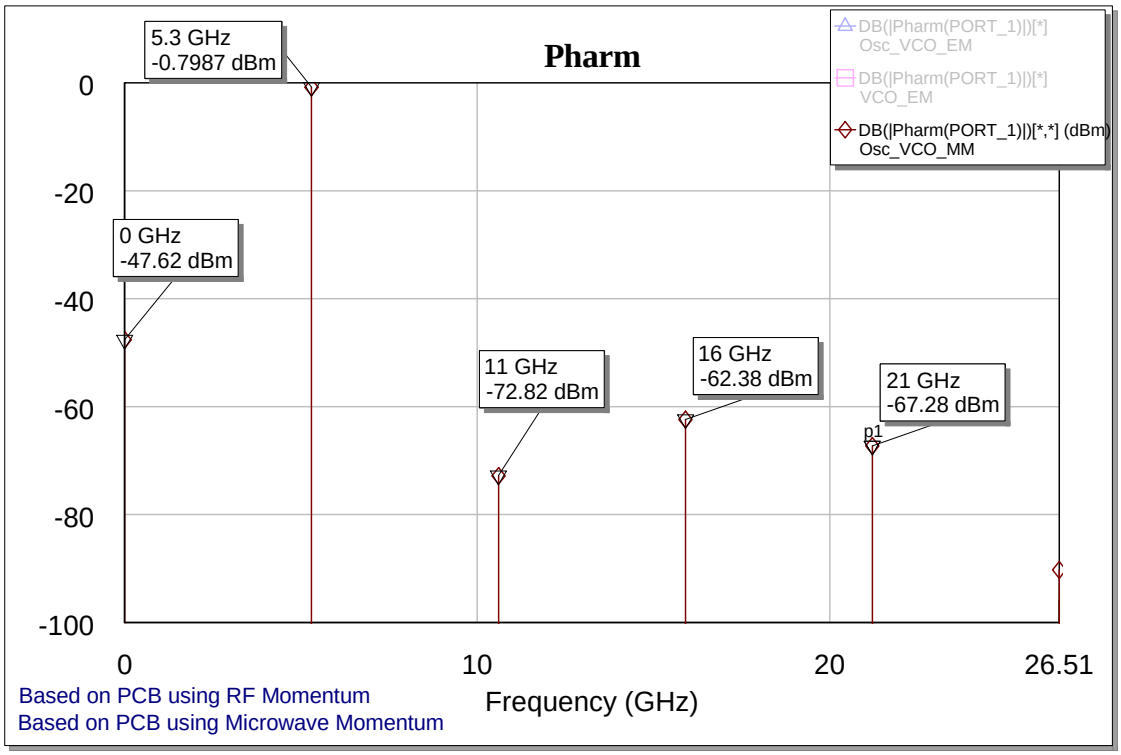

Figure 11: Spectral representation of the Oscillator

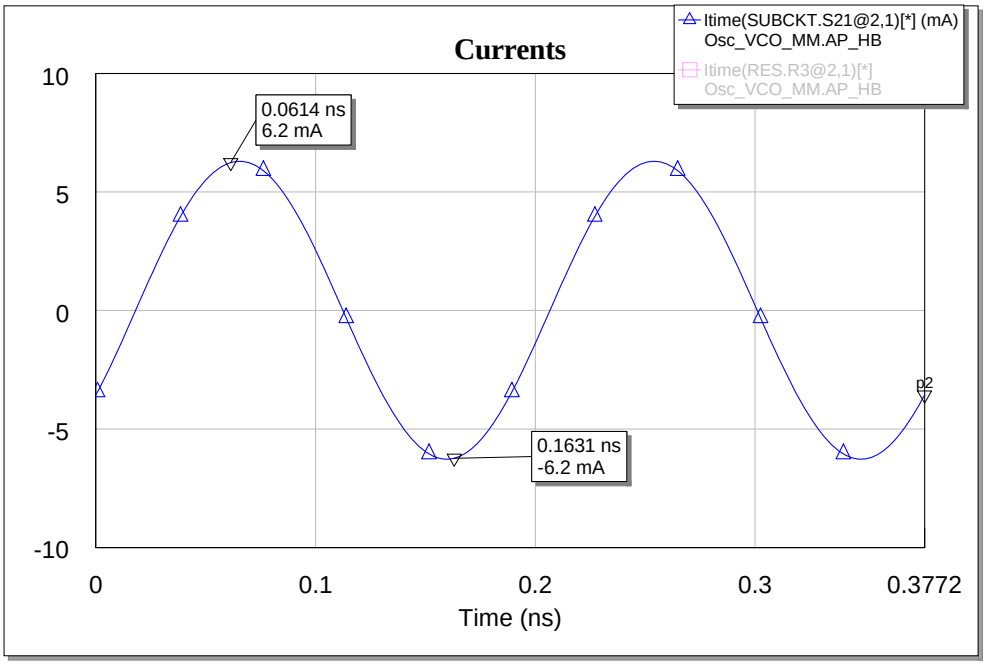

Figure 12: Output Current waveform for the oscillator

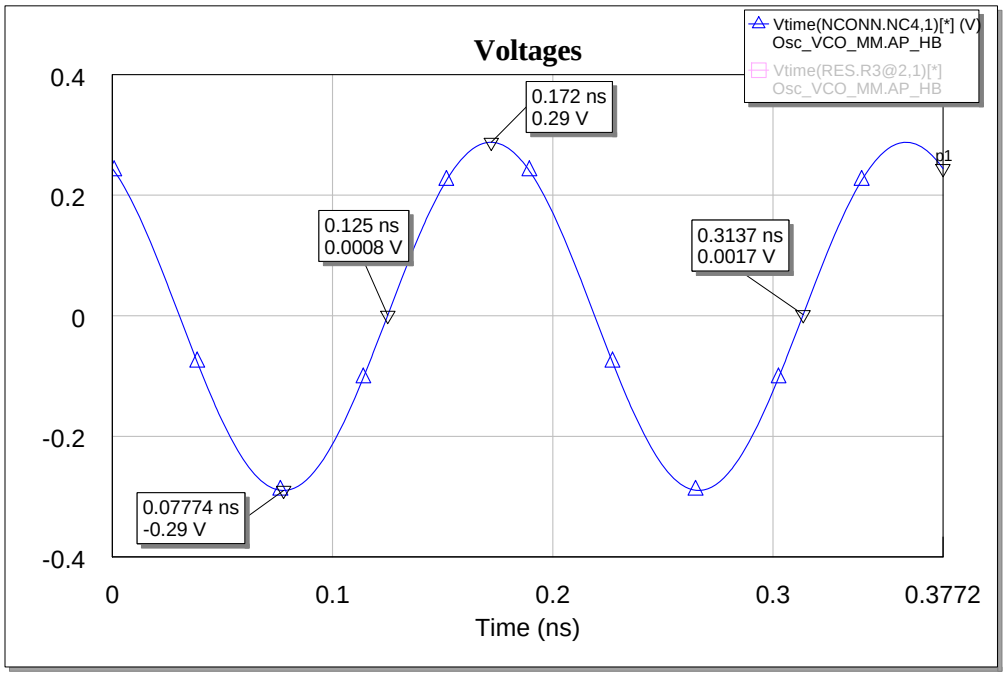

Figure 13: Output Voltage waveform for the oscillator

3.3.5 Oscillator performance Using the Simplified Oscillator Model

The simplified model in the AWR environment is shown in Figure 14.

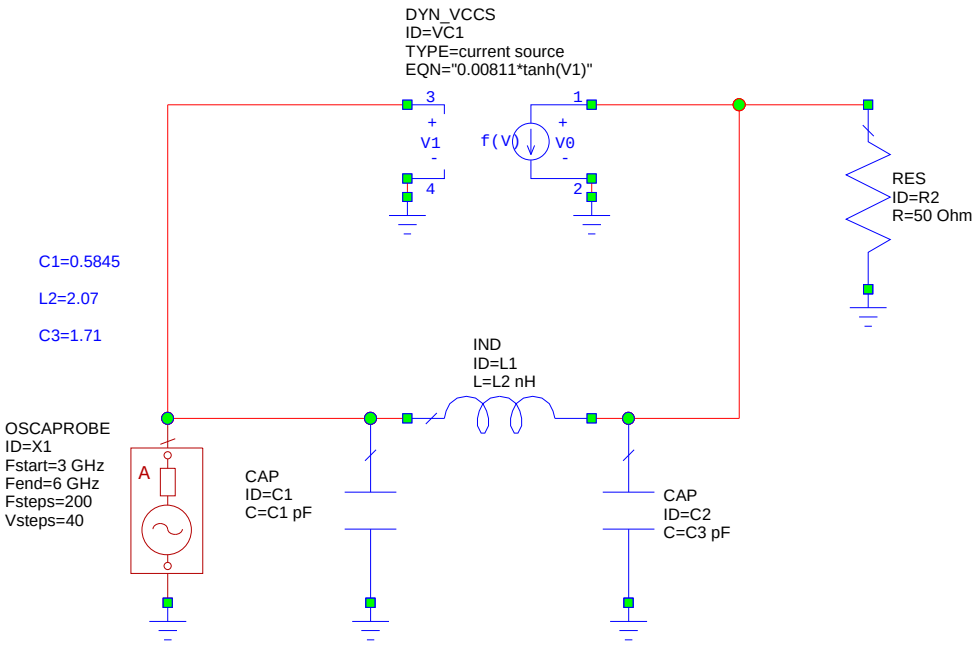

Figure 14: Schematic of the simplified oscillator model.

The key simulated results using the simplified model are shown in Figures 16 to 20. Figure 21 shows how the quantities plotted were measured.

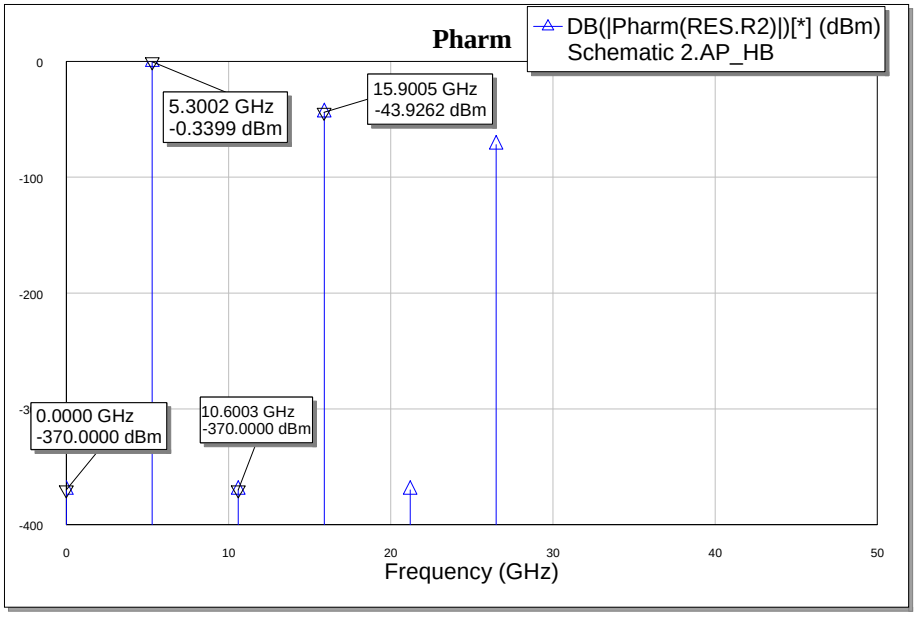

Figure 16: Spectral Representation of the simplified oscillator model.

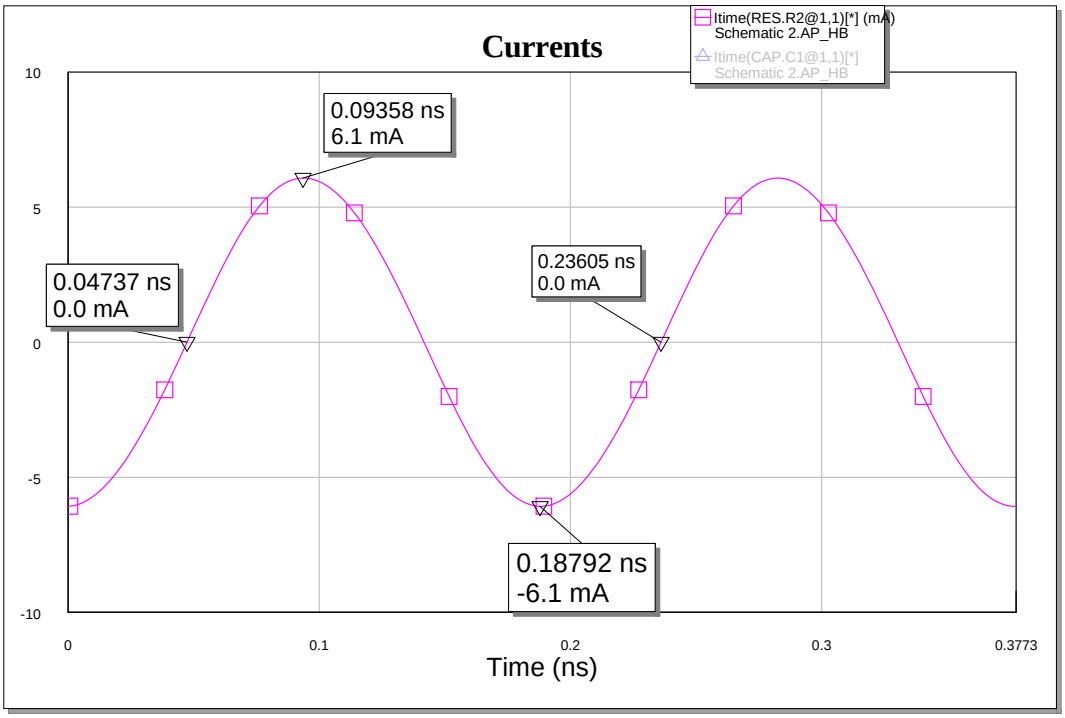

Figure 17: Output Current waveform for the simplified oscillator model.

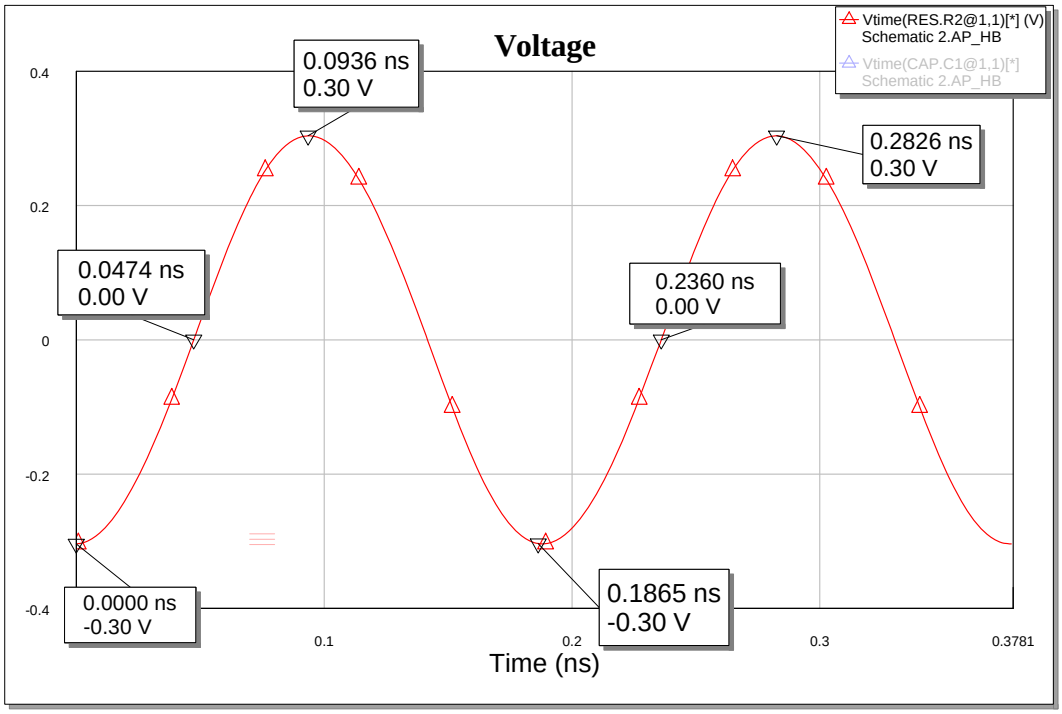

Figure 18: Output Voltage waveform for the simplified oscillator model.

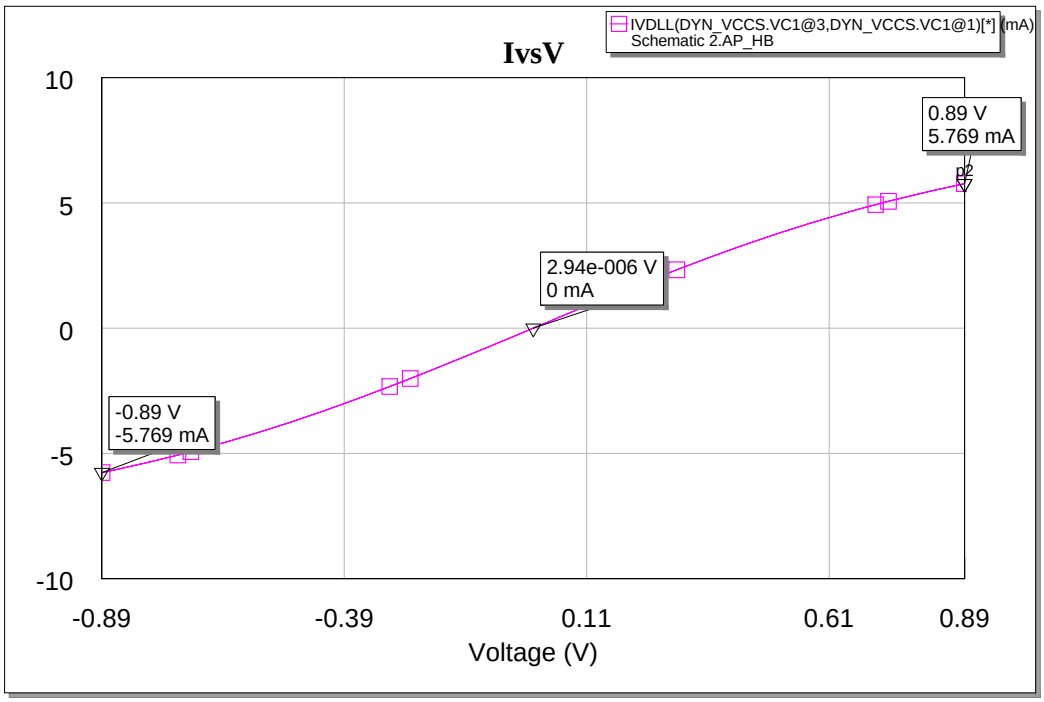

Figure 19: Transfer Function Plot, Output Current vs Input Voltage

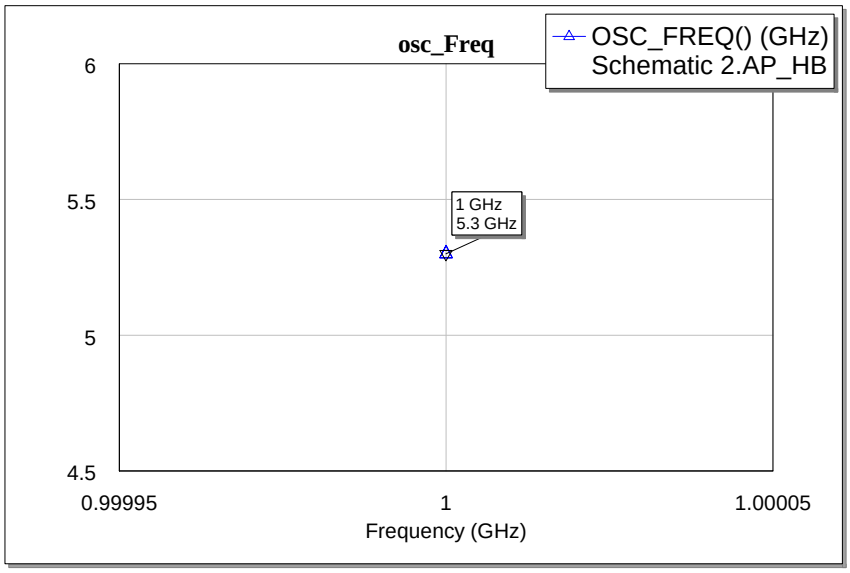

Figure 20: Determining the Frequency of oscillation

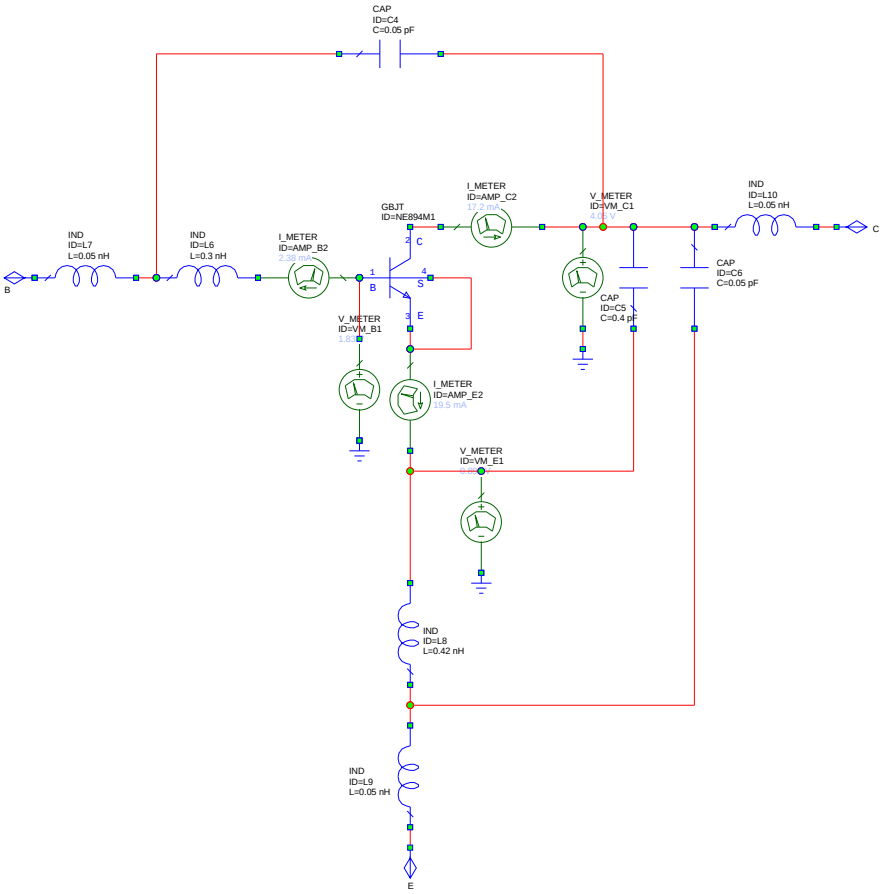

Figure 21: Measuring the terminal currents and voltages for the transistor

3.3.6 Summary

From the above AWR simulations of the voltage and current waveforms for the Complete Oscillator and the System Level Oscillator, we can confirm that the system level is a valid extraction of the complete oscillator. The required delay in the tanh function of the oscillator is 0.125 ns − 0.0474 ns = 77.6ps.

3.3.7 Oscillator Simulation in MATLAB

The simple oscillator model was simulated in MATLAB with the oscillating waveform shown in Figure 22.

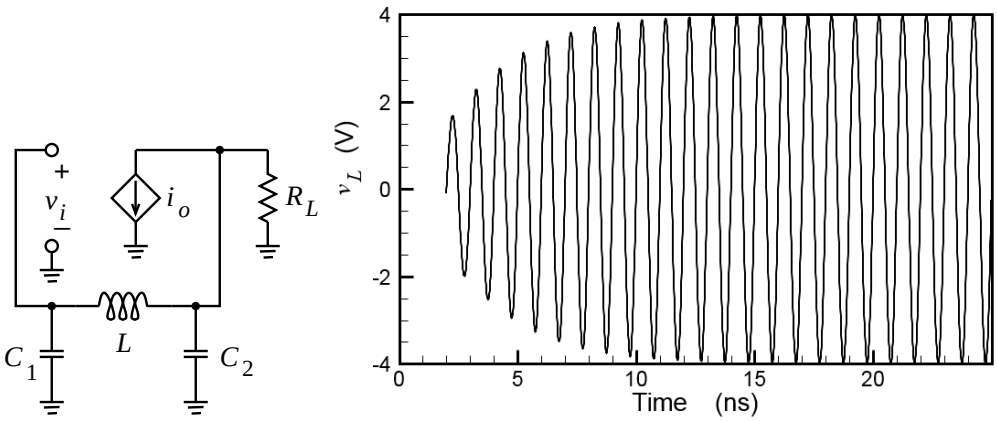

(a) (b)

Figure 22: A 1 GHz Colpitt's oscillator with start-up waveform: (a) minimum circuit; and (b) simulated transient response.

3.3.8 Phase Noise Investigations

One of the speculations for phase noise is that it could be due to time-delayed feedback around a weak nonlinearity — this produces chaotic behavior. A small computer program was written to model the Colpitt's osciallator circuit shown in Figure 23. The pi arrangement of capacitors and inductor ensures stable operation and the nonlinearity of the transconductance is modeled so that the output current is a tanh function of a time-delayed controlling voltage. Preliminary results are shown in Figure 24. These calculations were done using quad precision (double double precision in the C programming language). Quad precision must be emulated and so there is a significant increase in run time over simulation performed in normal double precision. Oscillation self-initiates and simulations are typically run for 10 million time points with the first 5 million discarded to remove transient effects. With so many time points efforts are required to minimize use of memory and ensure that the program remains in on-chip cache. One strategy we used was avoid the use of a fast Fourier transform. Instead discrete Fourier transforms at several discrete frequencies were performed by multiplying the calculated waveform at a particular time with the cos of the radian frequency times time and summing the result. It was necessary to perform the Fourier transformation in quad precision as well. All this results in a 3 to 5 day run time to produce the types of results shown in Figure 24. It takes considerable time to determine the optimum parameters including the time required to skip initial transients.

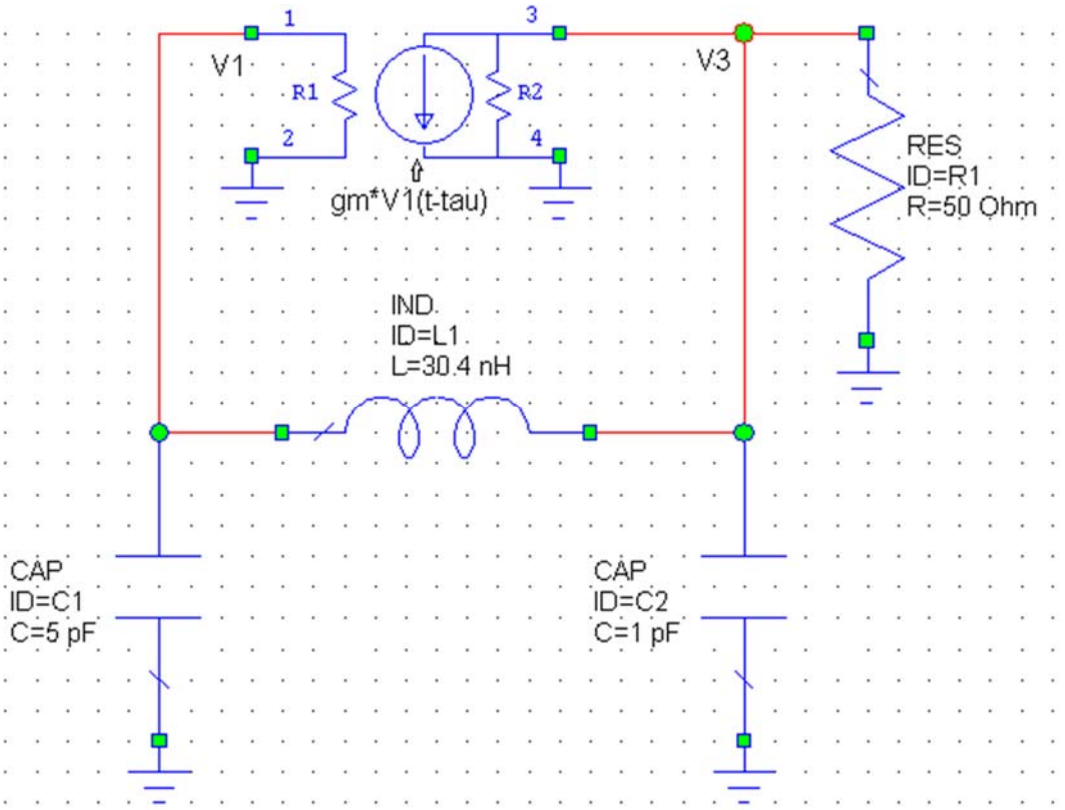

Figure 23: A Colpitts oscillator with a Colpitts feedback network (CLC) around a transconductance with a time-delay.

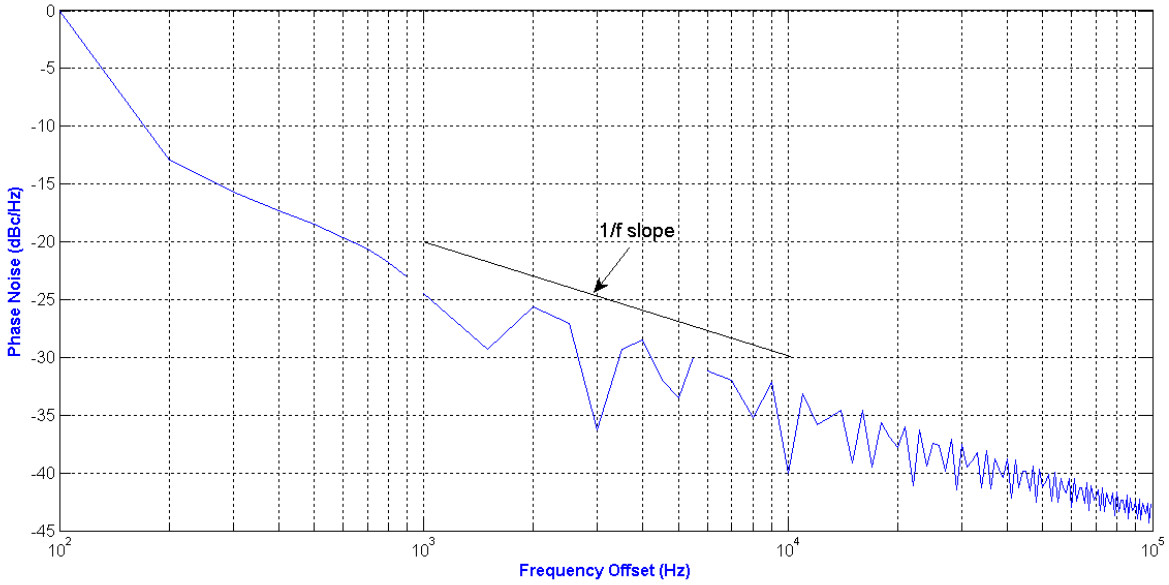

Figure 24: Plot of the phase noise of the Colpitts oscillator. Phase noise is normalized referenced to the phase noise at 100 Hz offset from the carrier and not strictly dB c (decibels with respect to the carrier).

One of the amazing results is the 1/*f* region of the phase noise curve shown in Figure 24. We have tried other nonlinear functions and this slope is still there. The phase noise level however is changed by varying the time delay. In Figure 24 there is also a hint that the phase noise has some higher slopes but many more points are required to do this. It appears that there could be a $1/f^2$ segment of the curve. Experimentally phase noise has been observed to have several $1/f^n$ regions where n ranges from 1 to 5 but is always an integer. Not all of these regions are observed however. The exciting thing will be to see if there are multiple $1/f^n$ regions captured in simulation for the same oscillator. If so then we have a reasonable idea of the ultimate source of phase noise. This could possibly lead to enhancements in our ability to build low noise oscillators. If we increase the number of points by a factor of 10 we are looking at run times of 20 to 30 days. Using a parallel computer does not have any affect as the program runs on a single core. We have spent approximately 5 months investigating how the simulations can run more quickly beginning with a MATLAB simulation. Using double precision arithmetic, which is hardware based speeds analysis up by about a factor of 20 but there is very little detail remaining.

3.3.9 Summary

The corresponding measured results are shown in Figure 25. The phase noise measured has many of the characteristics of the simple model simulated. Note that the simulated simplified model does not have a source of noise but it is known that a weakly nonlinear circuit with time-delayed feedback is a chaotic oscillator. The above results seem surprising but we were never able to convince ourselves that the results were nothing more than aliasing. Indeed some of our investigations showed that really could be aliasing. But why are the results so close. Could it be that the phase node measurement equipment (as well as the MATLAB simulations) is in fact simply reporting an aliasing result. This is even more complicated by the fact that the phase noise could be a chaotic signal. How does a phase noise measurement apparatus report the measurement of a chaotic signal. All this work was support by almost 1,000 hours of simulations but the more investigation done the more confusing the whole situation became.

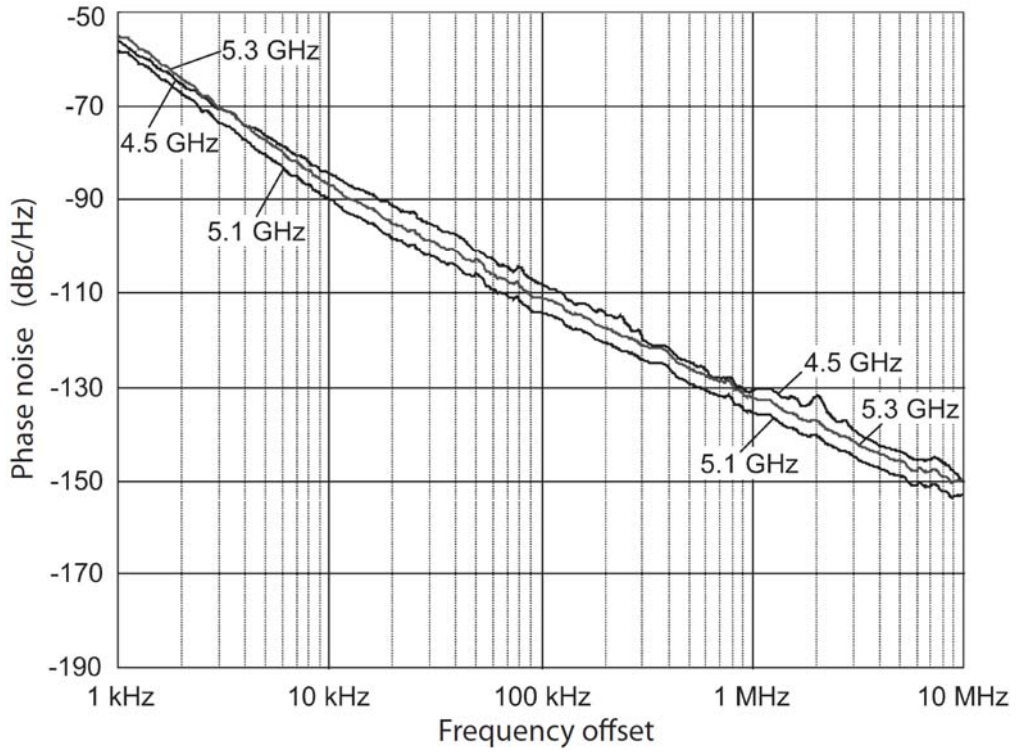

Figure 25: Phase noise measured at the top and bottom of the tuning range as well as at 5.1 GHz where phase noise is optimum. Minimum phase noise floor −116 dBc/Hz at 1 kHz offset, −160 dBc/Hz at 10 MHz offset.

4. Investigations of Spurious Signals introduced by a Vibrating Antenna

4.1 Concept

A two-tone signal traveling on a microstrip transmission lines will eventually result in third-order distortion although ostensibly the system is linear. What occurs is analogous to what happens when two tones applied to an amplifier as shown in Figure 26. The figure shows the spectrum of two tones applied to the input of an amplifier and the spectrum at the output of the amplifier has the original two tones plus two additional smaller tones called the third-order intermodulation products. With PIM the third-order tones exist with what is ostensibly a linear system.

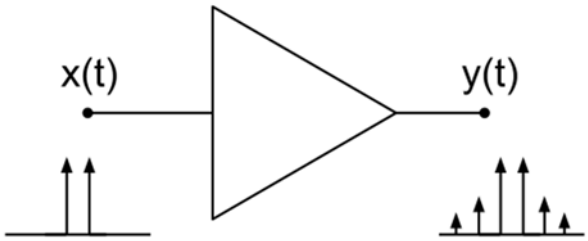

Figure 26. An amplifier showing the spectrum of a two-tone signal at the input (on the left) and a spectrum at the output (on the right) with two additional tones called third-order intermodulation produces.

Earlier measurements we performed on transmission lines and passive terminations are canonically shown in Figure 27. There are three distinct regions A, B and C. Our group was the first to be able to report measurements corresponding to regions A and B. It is now known that both regions are due to electrothermal effects with the breakpoint between regions A and B corresponding to the corner frequency of the lowpass thermal system. However the physical origins of region C are not known. We have undertaken measurements that seem to indicate the region C does not exist if there is a single metal-on-substrate transmission line system. We speculate that it may only occur when an adhesion metal is used. To explore this we have been collaborating with the University of Surrey who have excellent metallization capabilities. Our earlier attempts to create a silver line on a sapphire substrate resulted in lines that were only stable for a few days before delaminating. This is not surprising and this is why adhesion layers such as chrome are used. The adhesion layer is very thin but even so we believe that the different work functions in the two metal system are enough to result in distortion producing the region identified as C in Figure 27. Our intent is to characterize the PIM performance of a single metal transmission line and compare it to the characteristics of a transmission line with an adhesion layer. The tricky part of this is having a silver conductor on sapphire that does not delaminate. We have been getting ready for this experiment by increasing the stability and dynamic range of our PIM measurement system and conducting experiments with trial structures produced by the University of Surrey. Figure 5 shows a silver on sapphire test structure. We have wire-bonded to structures and have done simple pull tests. After one month no delamination was apparent. The complete transmission line system is now in fabrication.

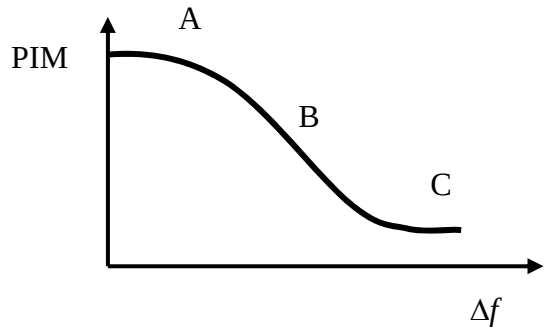

Figure 27: Plot of passive intermodulation distortion (PIM) versus tone spacing in a two-tone test.

4.2. Papers

The work done in this part of the project is documented in two published papers.

1. I. Kilgore, J. Wetherington, and M. B. Steer, Algorithmic strategies for high dynamic range analog cancellation," Government Microcircuit Applications Conf. (GOMACtech), March 2015.
2. I. M. Kilgore, S. A. Kabiri, A. W. Kane, M. B. Steer, "The effect of chaotic vibrations on antenna characteristics," *IEEE Antennas and Wireless Propagation Letters*, Vol. 15, 2016, pp. 1242–1244
3. I. M. Kilgore, A. W. Kane, S. A. Kabiri, and M. B. Steer, Analysis of RF interference resulting from antenna vibration," Government Microcircuit Applications Conf. (GOMACtech), March 2016.

The first paper describes modifications to a small signal measurement capability. This describes a measurement system for measuring small signals that only requires knowledge, i.e. measurement, of power and not amplitude and/or phase. This we believed was very important in measuring small signals. The second and third papers describe application of the measurement system to signals reflected by an antenna. Here a 900 MHz signal was fed and transmitted by an antenna. The small signal measurement system measured the signals coming back from the antenna. Additional content was added due to a special relativity effect. Doppler is special case of the effect. The reader is referred to the papers for a complete description. What is shown in the figures below are photos of the apparatus used as these photos are not in the published papers.

Figure 28 shows the antenna mounted on the vibration table. This is a $150 vibration table which is sold for high school experiments and costs around $150. The table exhibited chaotic vibrations as reported in the cited paper. A laboratory grade vibration table costing thousands of dollars does not exhibit chaotic vibrations. The vibration table uses what looks like a speaker coil which was driven by us at 100 Hz) to induce vibrations in the antenna. The antenna vibrations were measured by a laser Doppler vibrometer.

Figure 28: Monopole antenna attached to a vibration table.

The spectrum of the reflected RF signal from the antenna is shown in Figure 29. Spurious frequencies are seen at 100 Hz intervals. Using a doppler model we expect that these spurious signals levels to roll off linearly with respect to frequency away from the center frequency however a long tail was actually observed. There are other indications that the Doppler effect model is not a complete model including the asymmetric response observed. Another possibility is that additional harmonics present in vibration source, but we measured with an LDV and the vibration harmonics are 30 to 40 dB down.

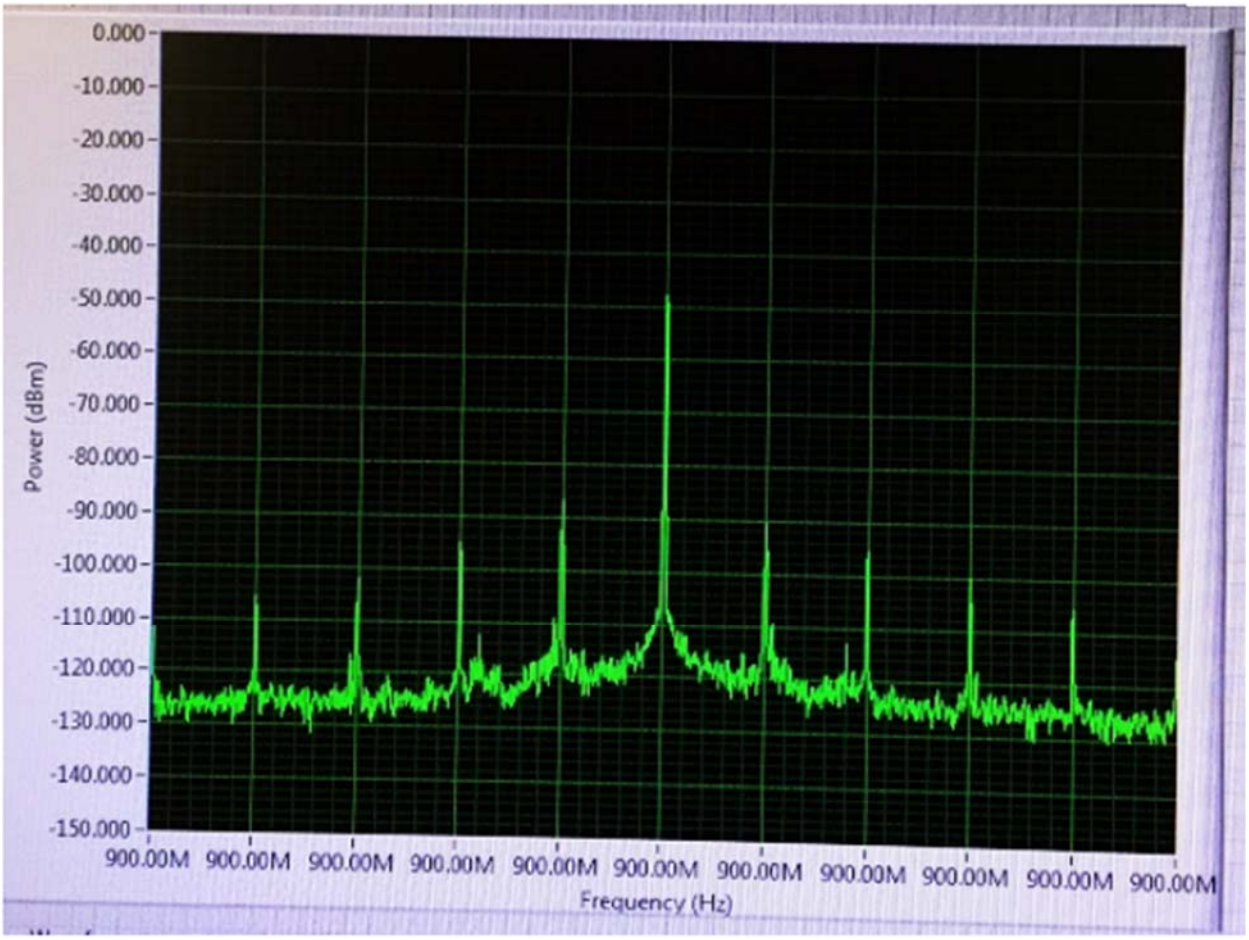

Figure 29: Signal "reflected" from vibrating antenna with 1 kHz span. The center frequency is at 915 MHz and was suppressed through cancellation. (Measurement system parameters: Carrier frequency 915 MHz; reference Level: -10 dBm; Signal generator power: -5 dBm; DUT power: -20.33 dBm; cancelled power: -62.06 dBm; Cancellation achieved: 41.73 dBm; Measurement noise floor: -115 dBm; measurement system dynamic range: 95 dB.

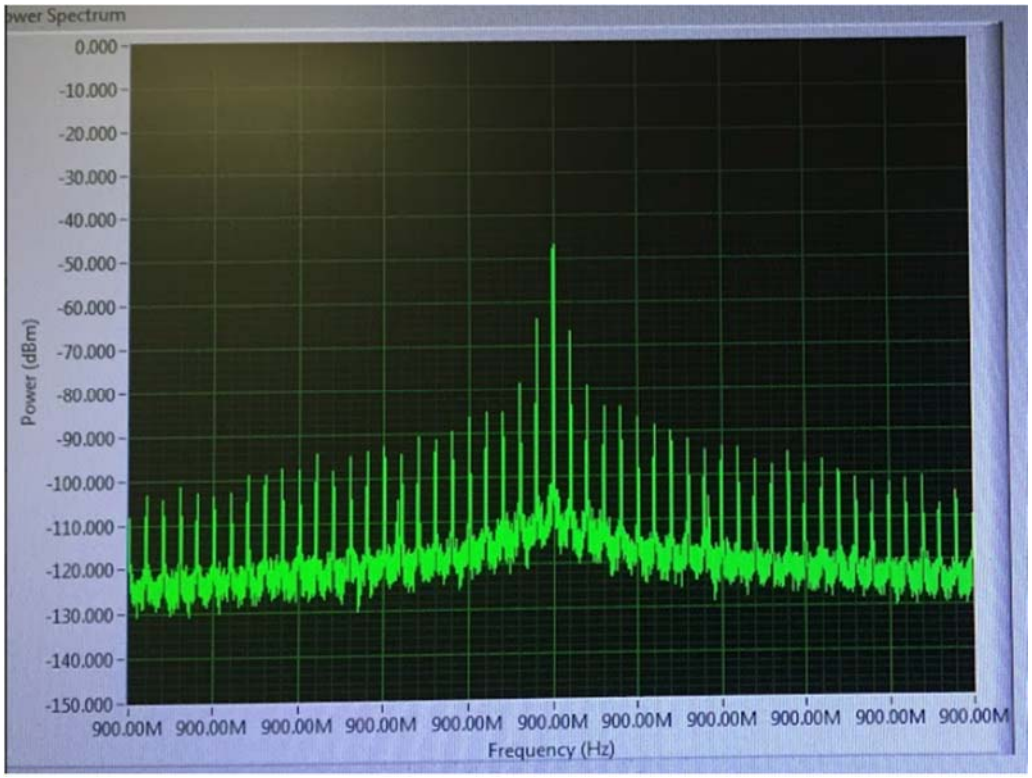

Figure 30: Signal "reflected" from vibrating antenna with 5 kHz span.

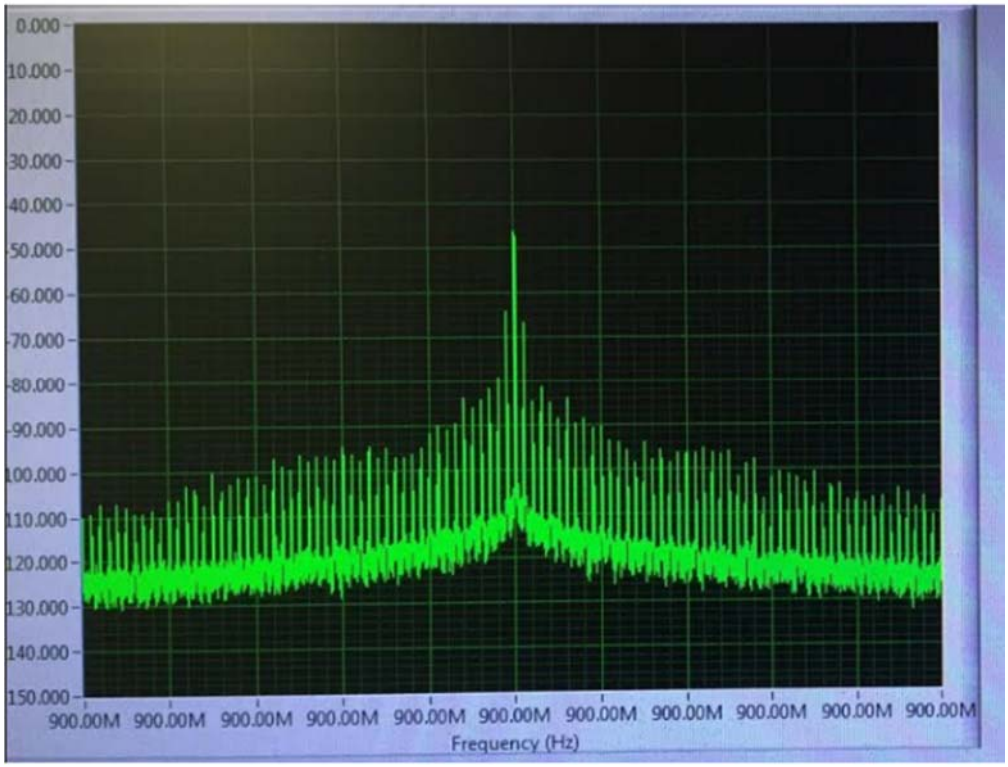

Figure 31: Signal "reflected" from vibrating antenna with 10 kHz span.

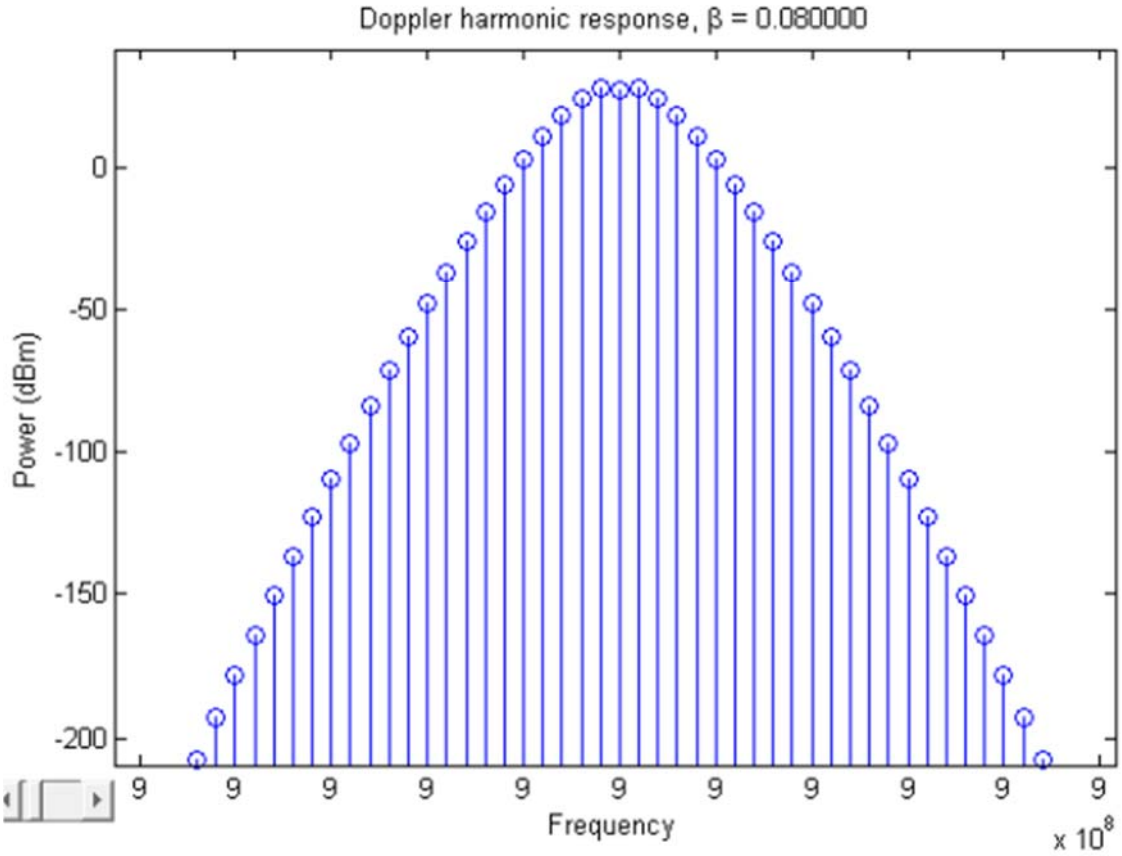

Figure 32: Expected roll off using Doppler model. This used the amplitude of the vibrations recored by the LDV at corresponding mechanical vibration frequencies.

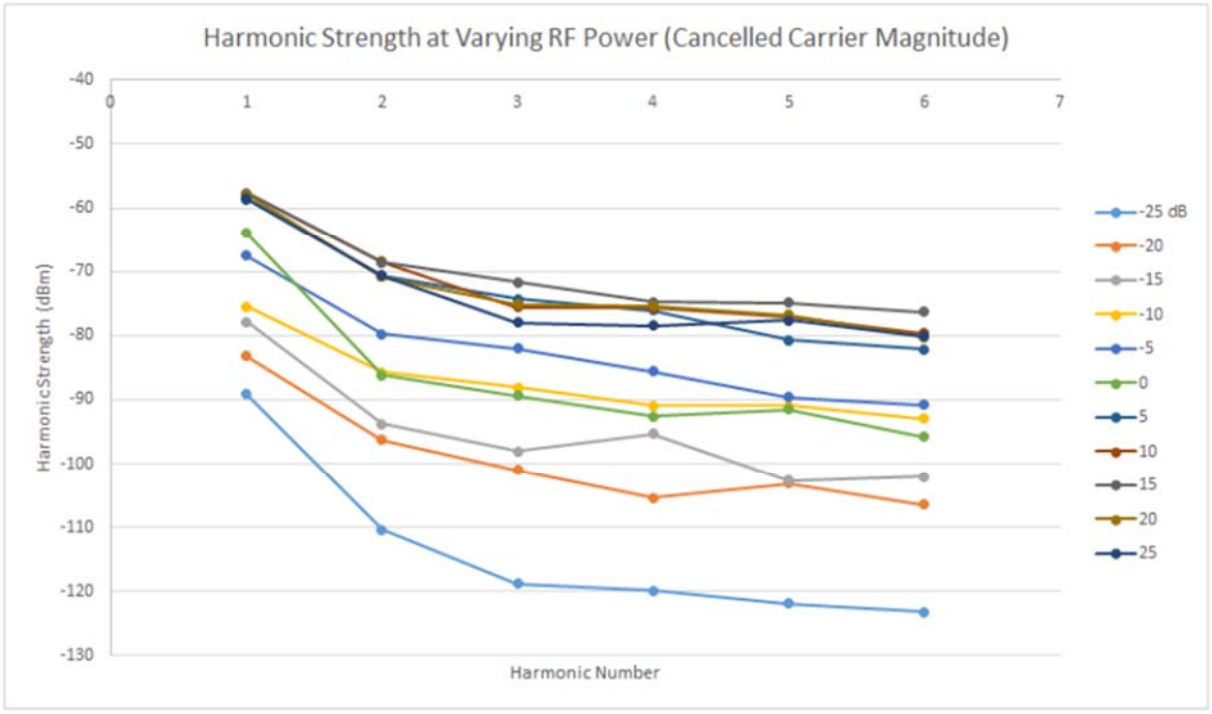

Figure 33: Magnitude of reflected RF response at frequencies offset at harmonics of 100 Hz.

Antenna vibrations were also induced using a studio speaker which provided more consistent (but less powerful) vibrations at lower frequencies. See Figure 34. The collection of recorded responses are in Figures 35 to 39.

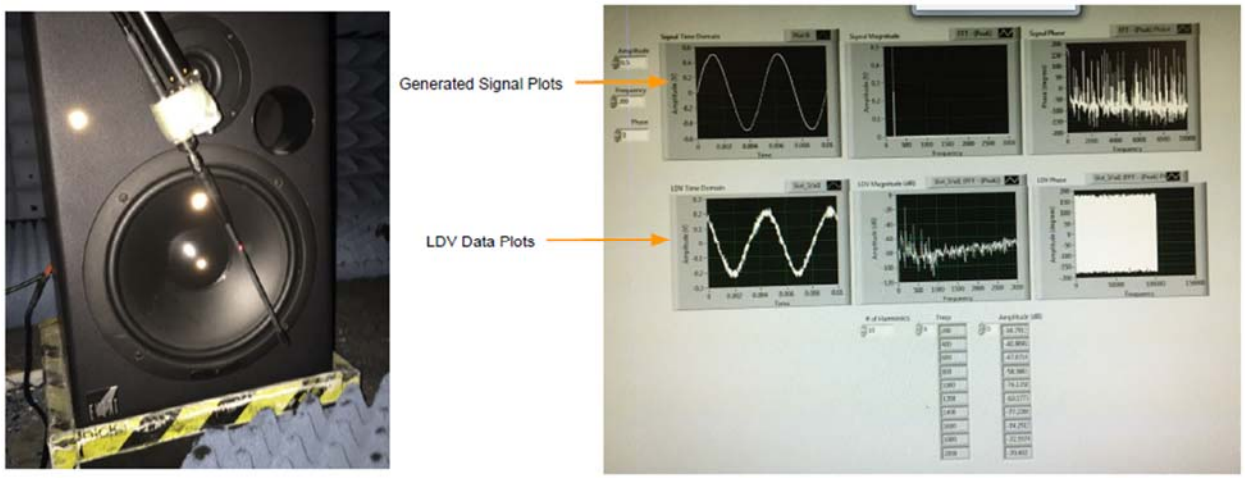

Figure 34: Acoustically excited vibrations.

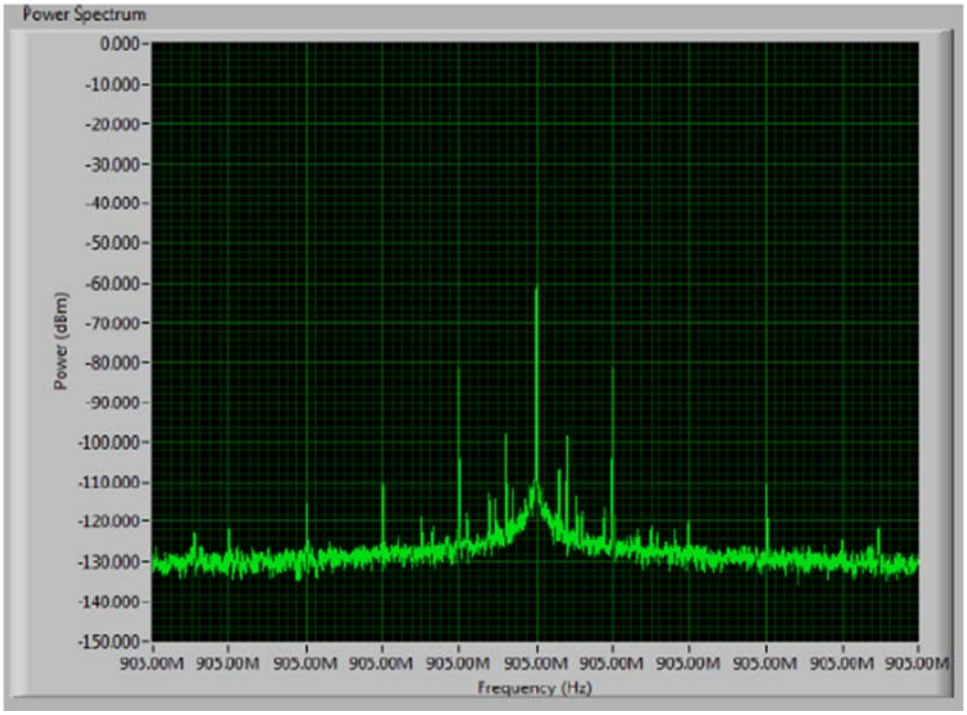

(a) acoustic source on

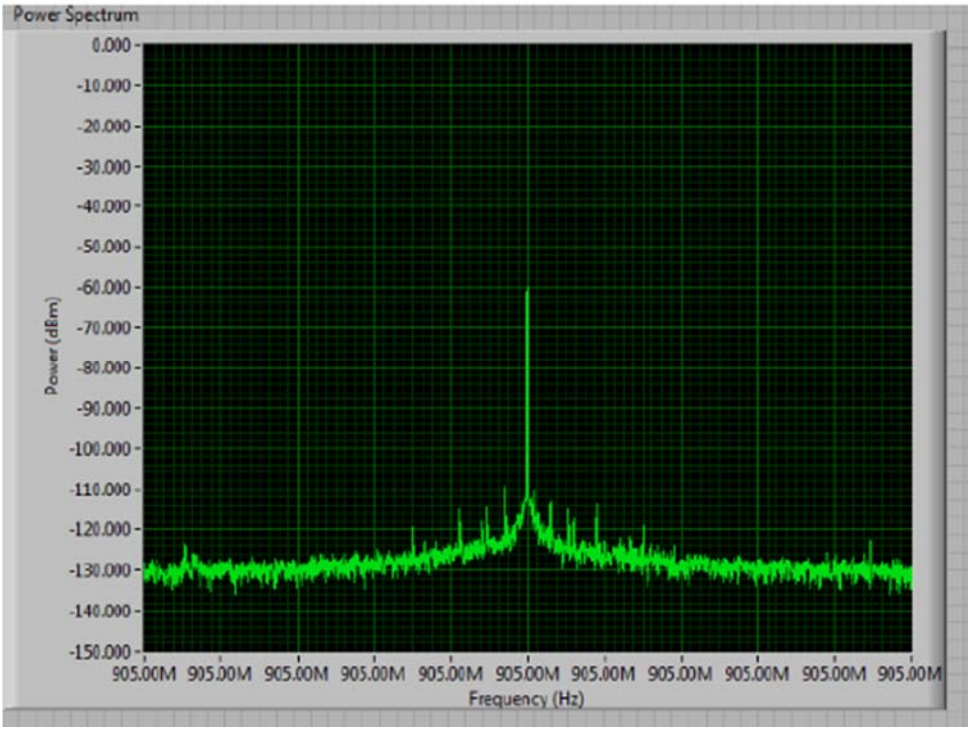

(a) acoustic source off

Figure 35: Measured "reflected" spectrum with speaker-induced (acoustic) vibrations.

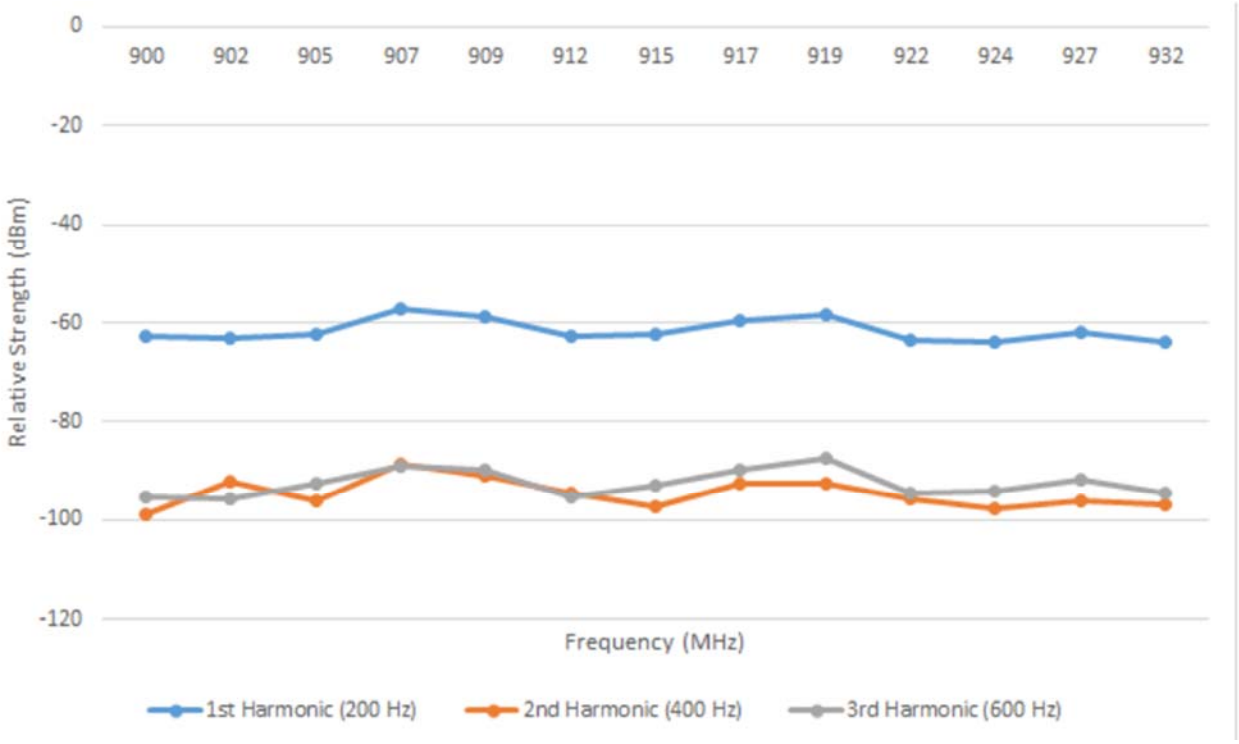

Figure 36: Relative sideband levels with acoustically excited vibrations.

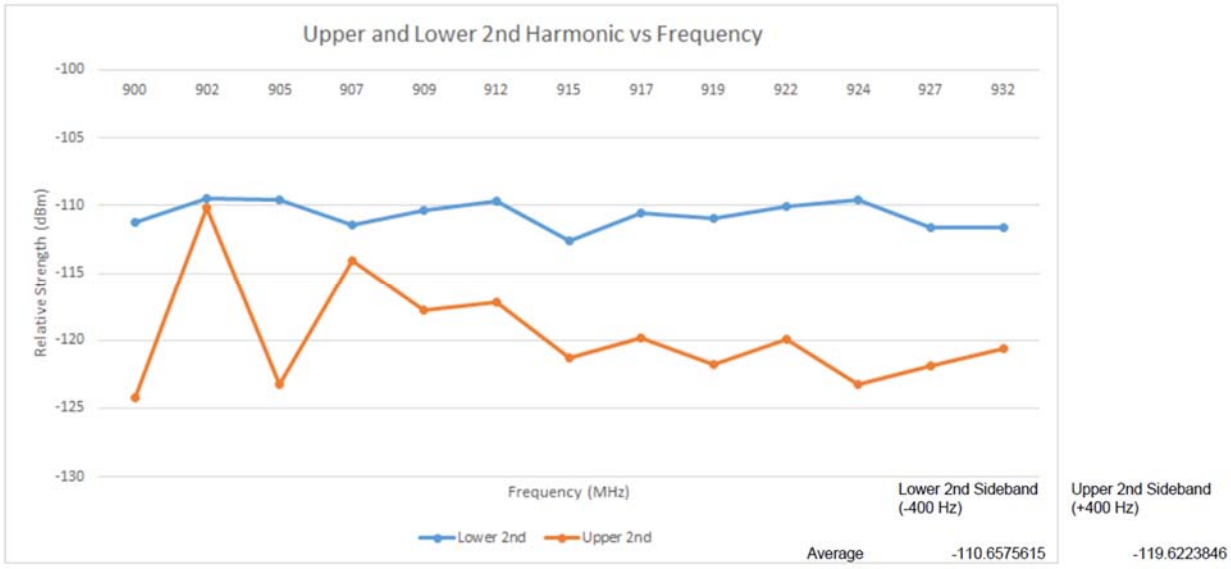

Figure 37: Asymmetric sidebands of acoustically stimulated vibrations.

Single tone incident on a vibrating surface =
FM -

$$\sum_{n=-\infty}^{\infty} J_n(k_{RF}\beta)cos([\omega_c + n\omega_v]t)$$

FM signal incident on vibrating surface -

$$\sum_{n=-\infty}^{\infty}\sum_{k=-\infty}^{\infty} J_k(m)J_n(k_{RF}\beta)cos([\omega_c + n\omega_v + k\omega_o]t)$$

Figure 38 : Frequency modulation formulas.

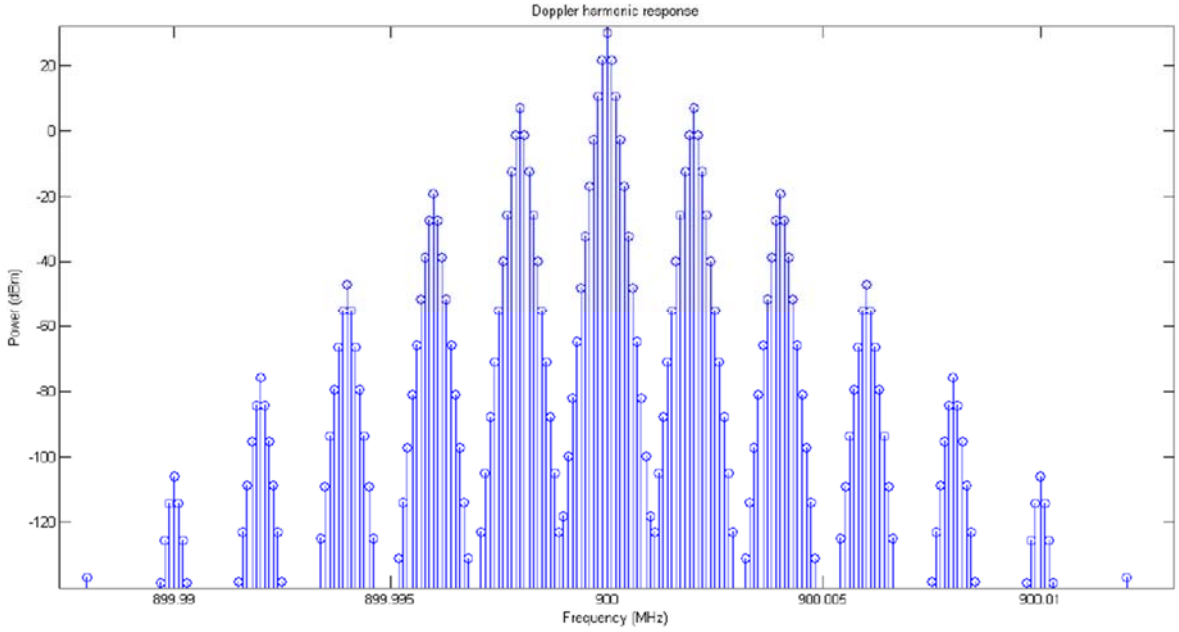

Figure 39: Calculated response obtained assuming a single-tone FM response. That is, a single tone incident on a vibratiing surface.

5. Recommendation for Follow-on Work

5.1 Summary

Follow-on work to this project should be less aggressive, and focus on developing investigative situations where the nonlinear dynamic behavior is exaggerated so that it can be captured by a real time oscilloscope which of courses has a reasonably low dynamic range. The equivalent analog dynamic range of a real time oscilloscope is DR = (6.02 x Q) (dB). Where Q is the number of bits. For a typical 8-bit real time oscilloscope this is 48 dB. This compares to the dynamic range of the frequency domain measurement system used with a dynamic range exceeding 100 dB.

Much work is left to be done. There is clearly unusual behavior, for example, the paper on vibrating antennas could actually provide the missing insight into way co-site interference problems are so intractable. Some of the work addressed in this report include oscillator phase

noise investigations. Phase noise of an oscillator is 20 to 30 dB higher than can be predicted using conventional analysis. Our premise was that perhaps the origin of phase noise was chaos. This proved to be too difficult a problem to look as phase noise is small and computational analysis required excessive analysis times. Even though this project is over work continues and here the so-called Chua circuit which produces large levels of chaotic behavior should be used in the analysis of phase noise. The signals in this circuit can be captured using a real time oscilloscope as well as requiring modest simulation times.

What also remains to be done is analysis of the ability to detect non-stationary signals, such as a chaotic signals, using our current measurement equipment which uses a stationary assumption. One of the issues that came up in this work is whether a spectrum analyzer or a phase noise meter is capturing the power in a nonstationary signal. One line of thinking is that is does not. This is a project in its own right and was just part of the project being reported on.

5.2 Specific topic of future investigation are:

1. Does a modern spectrum analyzer have aliasing errors.
2. In spectrum analyzers for 20 or more years ago a narrow bandpass filter, a YIG tuned sphere, was used to pass only signals in a very narrow band. A bandpass filter is a correlator and so it would treat noise differently than a correlated signal. What is the impact on the signal level reported.
3. Investigate phase noise of a noisy oscillator with high-level noise. An example is the Chua circuit that oscillates chaotically and the levels of chaos are large. Presumably this would enable rapid simulations and aliasing problems in the reported results can be minimized or at least understood. In effect this is a strategy of exaggerating an effect so that it can be more easily studied.
4. Construct an RF noisy circuit and investigate using a high frequency real time oscilloscope.
5. Analyze the reflected signals from a vibrating antenna using a high-speed real time oscilloscope.
6. Modify tools for the analysis of signals with nonlinear dynamics. A chaotic signal is an example of such signals. Current tools seem to be focused on large-scale chaotic effects and proved not to be robust for low level signals in the presence of large signals.